
THE LIPSCHITZ-VARIANCE-MARGIN TRADEOFF FOR ENHANCED RANDOMIZED SMOOTHING

Blaise Delattre^{1,2}, Alexandre Araujo³, Quentin Barthélémy¹ and Alexandre Allauzen^{2,4}

¹ FOXSTREAM, Vaulx-en-Velin, France

² Miles Team, LAMSADE, Université Paris-Dauphine, PSL University, Paris, France

³ Department of Electrical and Computer Engineering, New York University, USA

⁴ ESPCI PSL, Paris, France

ABSTRACT

Real-life applications of deep neural networks are hindered by their unsteady predictions when faced with noisy inputs and adversarial attacks. The certified radius is in this context a crucial indicator of the robustness of models. However how to design an efficient classifier with a sufficient certified radius? Randomized smoothing provides a promising framework by relying on noise injection in inputs to obtain a smoothed and more robust classifier. In this paper, we first show that the variance introduced by randomized smoothing closely interacts with two other important properties of the classifier, *i.e.* its Lipschitz constant and margin. More precisely, our work emphasizes the dual impact of the Lipschitz constant of the base classifier, on both the smoothed classifier and the empirical variance. Moreover, to increase the certified robust radius, we introduce a different simplex projection technique for the base classifier to leverage the variance-margin trade-off thanks to Bernstein’s concentration inequality, along with an enhanced Lipschitz bound. Experimental results show a significant improvement in certified accuracy compared to current state-of-the-art methods. Our novel certification procedure allows us to use pre-trained models that are used with randomized smoothing, effectively improving the current certification radius in a zero-shot manner.

1 INTRODUCTION

Deep neural networks are highly susceptible to adversarial attacks, which are small, carefully crafted perturbations that lead the model to make erroneous predictions (Szegedy et al., 2013). This vulnerability is a critical concern in applications requiring high reliability and safety, such as autonomous vehicles and medical diagnostics. Various defense mechanisms, including certified defenses like Lipschitz continuity (Tsuzuku et al., 2018) and randomized smoothing (Cohen et al., 2019), have been proposed to mitigate these risks. Among the metrics used to evaluate these defenses, the certified robust radius serves as an important measure for quantifying model resilience against adversarial perturbations (Tsuzuku et al., 2018). The certified robust radius measures the amount of perturbation that can be added to an input x , while keeping the stability of the decision y , *i.e.* the label in a classification task. This essentially acts as a certified measure of robustness for an individual input. Similarly, the prediction margin acts as an indicator of the classifier’s confidence in assigning the label y to the input x . A larger prediction margin correlates with an increased confidence in the prediction, even if the input incurs some perturbations.

The concept of Lipschitz continuity augments this framework by introducing the Lipschitz constant which bounds the sensitivity of the *base classifier* to input perturbations. A smaller Lipschitz constant signifies that the function *base classifier* exhibits slower variations in its output with respect to changes in its input, inherently contributing to the robustness of the classifier. Tsuzuku et al. (2018) gathers these elements to provide a bound on the certified robust radius that encompasses both the prediction margin and the Lipschitz constant. This combined measure controls the trade-off between the classifier’s prediction margin and its sensitivity to input changes. Upon the introduction of randomized smoothing (RS), Cohen et al. (2019); Salman et al. (2019); Levine et al. (2020) use the *smoothed classifier* obtained by convolving Gaussian density with the *base classifier*. Salman

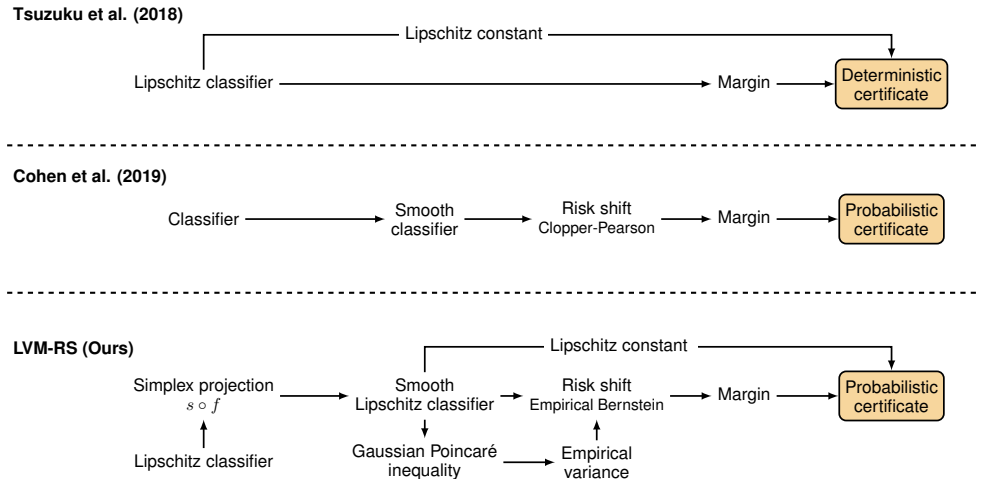


Figure 1: **First**, Tsuzuku et al. (2018) proposes a deterministic certificate starting from a Lipschitz *base classifier*, followed by margin calculation and radius binding. **Second**, Cohen et al. (2019) introduces a *base classifier* to create a *smoothed classifier*. The risk factor α is then estimated using the *Clopper-Pearson* interval to provide a probabilistic certificate. **Third**, our method (the *Lipschitz-Variance-Margin Randomized Smoothing* or LVM-RS) extends a smoothed classifier constructed with a Lipschitz base classifier with simplex projection. The regularization of the Lipschitz constant is motivated by the Gaussian-Poincaré inequality in Theorem 1. The empirical variance is applied to the Empirical Bernstein inequality in Proposition 2 to accommodate for the risk factor α , in the same flavor as in Levine et al. (2020). The pipeline also ends with a probabilistic certificate, similar to the methodology used in Cohen et al. (2019)’s certified approach.

et al. (2019) proved that the *smoothed classifier* exhibits Lipschitz continuity which depends on the Gaussian variance. RS methods estimate a *smoothed classifier* by injecting noise on the input. The resulting procedure is then probabilistic and approximate inference is carried out with Monte-Carlo (MC) methods. To account for the randomness introduced through MC, one can use an α -level confidence interval (*Pearson-Clopper*) as in (Cohen et al., 2019; Salman et al., 2019), or concentration inequality (*Hoeffding’s inequality*) as in (Lecuyer et al., 2019; Levine et al., 2020) to control the risk induced by the randomness. A shift is thus necessary to lower-bound the prediction margin, thus yielding a more conservative but also more reliable estimate of the robust radius.

In the last step of traditional classification, the decision usually relies on the argmax function. This can be seen as a projection of the network’s output, putting all the probability mass on one corner of the simplex. However, in the context of RS, there is a detour: RS or the smoothed classifier conducts an argmax projection on the expectation of the argmax applied to the base and deterministic classifier.

In this work, we revisit the whole decision process of RS to better leverage and disentangle the interplay of all these ingredients. We propose to better leverage the margin variance tradeoff with alternative simplex projections. More importantly, we investigate how Lipschitz regularity impacts randomized smoothing techniques, emphasizing its effects on the certified robust radius. There is a circular dependency: the regularity of the *smoothed classifier* depends on the Lipschitz property of the *base classifier* and the variance of the Gaussian convolution which governs the induced level of smoothness. Therefore, our research in this domain encompasses four contributions:

- We use the *Gaussian-Poincaré Theorem* to explain the impact of the Lipschitz constant of the *base classifier* on MC variance, which ultimately affects its reliability, see Section 3.2.
- We introduce the use of the *Empirical Bernstein inequality* which integrates empirical variance to control risk α , see Section 3.3.
- We present the *Lipschitz-Variance-Margin Randomized Smoothing* (LVM-RS) procedure, presented in Figure 1, which balances MC variance and decision margin and controlled the

MC empirical variance through the different simplex projections. This procedure demonstrates state-of-the-art results on the CIFAR-10 and ImageNet datasets, see Section 3.5.

- We establish a novel limit on the Lipschitz constant for the *smoothed classifier*, detailing its reliance on both noise variance and the *base classifier*'s Lipschitz constant, whilst clarifying the correlation between robustness certificates produced through Randomized Smoothing and the one from deterministic approaches as in Tsuzuku et al. (2018), see Section 3.4.

2 BACKGROUND & RELATED WORK

The robustness of machine learning classifiers remains an area of active research, with various strategies being proposed and evaluated. In this section, we touch upon significant contributions in the domains of Lipschitz-based robust classifiers, randomized smoothing, and the role of margins in the robustness of classifiers.

2.1 NOTATION

Consider a d -dimensional input data point $x \in \mathcal{X} \subset \mathbb{R}^d$ and its associated label $y \in \mathcal{Y} = \{1, \dots, c\}$, where \mathcal{Y} encompasses c distinct classes. The $(c-1)$ -dimensional simplex is defined as $\Delta^{c-1} = \{p \in \mathbb{R}^c \mid \mathbf{1}^\top p = 1, p \geq 0\}$ and let $s : \mathbb{R}^c \mapsto \Delta^{c-1}$ denote the projection onto this simplex. Frequently, the projection s corresponds to the softmax or argmax projection.

For a logit vector $z \in \mathbb{R}^c$, its projection on the simplex is denoted by $s(z)$. This projection can use a temperature t such that $s^t(z) = s(z/t)$. For instance the argmax corresponds for the component k as $s_k(z) = \mathbb{1}_{\arg \max_i z_i = k}$ which puts all the mass on the maximum value coordinate. This projection can be obtained through softmax with low temperature $t \rightarrow 0$. A function $f : \mathcal{X} \mapsto \mathbb{R}^c$ is designated as the subclassifier before the projection s . The main classifier can be formulated as $F(x) = \arg \max_{k \in \mathcal{Y}} s_k(f(x))$, resulting in the predicted label $\hat{y} = F(x)$. While F offers predictions for an input x , it doesn't convey the confidence level associated with these predictions; such information is furnished by f .

The margin of safety surrounding a classifier's decision boundary for a particular input x is captured by the certified radius, denoted as $R(f, x)$. This radius represents the maximum permissible level of perturbation, ϵ , that can be introduced to input x without altering its classification output to remain consistent with its true label. A larger certified radius is indicative of a classifier's robustness against input perturbations. Its formal expression in the context of the ℓ_2 -norm is:

$$R(f, x) = \arg \max_{\epsilon} \left\{ \|\tau\|_2 \leq \epsilon \mid \arg \max_k f_k(x + \tau) = y \right\}.$$

As proposed by Tsuzuku et al. (2018), the prediction margin, $M(f(x))$, for a classifier f and an input x is: $M(f(x)) = \max(0, f_y(x) - \max_{k \neq y} f_k(x))$. For a function f that is Lipschitz continuous concerning the ℓ_2 -norm, its Lipschitz constant is represented as: $L(f) = \sup_{x \in \mathbb{R}^d} \|\nabla f(x)\|_2$. When f maintains element-wise Lipschitz continuity under the ℓ_2 -norm, the maximum element-wise Lipschitz constant is depicted by: $l(f) = \max_k L(f_k)$. In the following of the paper, we defer all proofs in Appendix A.

2.2 LIPSCHITZ CONTINUITY IN CLASSIFIER DESIGN

The concept of Lipschitz continuity has been recognized for its intrinsic value in designing robust classifiers. By ensuring that a function possesses a bounded Lipschitz constant, it can be ascertained that small perturbations in the input don't result in large variations in the output.

Proposition 1 (Tsuzuku et al. (2018)). *Given a Lipschitz continuous subclassifier f for the ℓ_2 -norm, and given a perturbation level $\epsilon > 0$, $x \in \mathcal{X}$, and $y \in \mathcal{Y}$ as the label of x . If the margin $M(f(x))$ at input x meets the condition:*

$$M(f(x)) > \sqrt{2}L(f)\epsilon,$$

then for every τ such that $\|\tau\|_2 \leq \epsilon$, we have $\arg \max_k f_k(x + \tau) = y$.

Reworking the above proposition, the certified radius for a subclassifier f at x can be expressed as:

$$R_1(f, x) = \frac{M(f(x))}{\sqrt{2L(f)}}. \quad (1)$$

This inherent property positions Lipschitz continuity as a strong defense mechanism against adversarial attacks. Recent efforts have focused on creating Lipschitz by design classifiers, incorporating Lipschitz constraints either during the training phase via regularization or through specific architectural designs Tsuzuku et al. (2018); Anil et al. (2019); Trockman & Kolter (2021); Singla & Feizi (2021b); Meunier et al. (2022); Araujo et al. (2023); Wang & Manchester (2023). Some works (Araujo et al., 2021; Singla & Feizi, 2021a; Delattre et al., 2023) provide soft Lipschitz constant regularization of individual layers. However, there is a trade-off between the Lipschitz of the network and performance for the same level of margins, as depicted in (Béthune et al., 2022, Appendix N). Non-deterministic and smoother approaches enjoy better performance but are costly as they have heavy sampling procedures.

2.3 RANDOMIZED SMOOTHING

RS has positioned itself as a compelling methodology to procure certified robustness in classifiers. The central philosophy is to introduce Gaussian noise into inputs and, when averaged over, results in an estimated smoother classifier with increased resilience against adversarial inputs. The seminal work of Cohen et al. (2019) laid the foundation for RS, showcasing its ability to achieve state-of-the-art certified robustness for ImageNet classifiers. This work was later augmented by Salman et al. (2019), who derived the bounds of the element-wise Lipschitz constant of the smoothed classifier, providing deeper insights into the potential and boundaries of RS. Randomized smoothing is applied to *base classifier* F to produce the *smoothed classifier* \tilde{F} :

$$\tilde{F}(x) = \arg \max_k \mathbb{P}_{\delta \sim \mathcal{N}(0, \sigma^2 I)}(F(x + \delta) = k) = \arg \max_k \mathbb{E}_{\delta \sim \mathcal{N}(0, \sigma^2 I)}[\mathbb{1}_{\arg \max_i f_i(x + \delta) = k}],$$

which can be generalized to any simplex projection s :

$$\tilde{F}_s(x) = \arg \max_k \mathbb{E}_{\delta \sim \mathcal{N}(0, \sigma^2 I)}[s_k(f(x + \delta))] = \arg \max_k \tilde{f}(x),$$

where s corresponds in this context to the argmax projection on the simplex, applied to the *base subclassifier* f through the RS process, Cohen et al. (2019); Salman et al. (2019).¹.

In the realm of randomized smoothing, both Cohen et al. (2019) and Salman et al. (2019) propose bounds on the certified radius. Specifically, these bounds are relevant for the composite classifier defined as $\Phi^{-1} \circ \tilde{f}$, where Φ^{-1} represents the quantile function of the Gaussian distribution:

$$R_2(\Phi^{-1} \circ \tilde{f}, x) = \frac{\sigma}{2} \left(\Phi^{-1}(\tilde{f}_{\hat{y}}(x)) - \Phi^{-1}(\max_{k \neq \hat{y}} \tilde{f}_k(x)) \right). \quad (2)$$

Note that $\Phi^{-1}(\max_{k \neq \hat{y}} \tilde{f}_k(x)) = \max_{k \neq \hat{y}} \Phi^{-1}(\tilde{f}_k(x))$ because Φ^{-1} is monotonically increasing.

The drawback of RS is the sampling cost, as it can require a large number of samples to perform randomized smoothing. To tackle this issue the work of Horváth et al. (2022) leverages ensemble classifiers to reduce variance and propose an adaptive sampling procedure to verify whether a target-certified radius is reached or not. In this work, we also aim at reducing variance.

2.4 MARGINS AND CLASSIFIER ROBUSTNESS

The margin, often conceptualized as the distance between the decision boundary and the closest data instance, serves as a pivotal component in classifier robustness. Larger margins are generally associated with better generalization capabilities, a foundational principle behind algorithms such as support-vector machines. In the context of adversarial robustness, margins play a crucial role, with various studies underscoring the relationship between margins and resilience against adversarial perturbations (Tsuzuku et al., 2018). Efforts to optimize for larger margins, combined with other robustness-enhancing strategies, have shown promise in bolstering classifier defense mechanisms.

¹Levine et al. (2020) do not use a simplex projection but normalized outputs in $[0, 1]$ for another task.

The work of Béthune et al. (2022) explores the link between margin maximization and Lipschitz continuity, and shows how both notions implement an accuracy-robustness trade-off.

While RS and Lipschitz continuity by design have predominantly been researched in their distinct capacities, recent inquiries hint at an inherent synergy between them and the key role of margins. Our exploration delves deep into this nexus, unraveling novel insights that can propel the development of future robust classifiers.

3 THE LIPSCHITZ-VARIANCE-MARGIN TRADEOFF

3.1 RELATION BETWEEN CERTIFIED RADII

In this subsection, our objective is to recast various certified radii as the ratio between a margin and a Lipschitz constant. Adopting this unified formulation facilitates comparisons across radii introduced in different research communities. A notable observation is that the robustness of a classifier can be deterministically certified using its Lipschitz constant. Calling $g = \Phi^{-1} \circ \tilde{f}$, the radius of R_2 of Equation (2) can be recast as:

$$R_2(g, x) = \frac{M(g(x))}{2l(g)} = \frac{M(g(x))}{\sqrt{2} \times \sqrt{2}l(g)}, \quad (3)$$

wherein $l(g) = \frac{1}{\sigma}$ represents the element-wise Lipschitz constant of g (Salman et al., 2019). Highlighting the element-wise Lipschitz constant, $l(g)$, enables us to bridge the gap between the two radii, R_1 and R_2 , $L(g)$ and $\sqrt{2}l(g)$ play the same role. Note that those radii can also be applied to $g = \tilde{f}$, Salman et al. (2019) derived bound for $l(g)$ in that case.

Most of the randomized smoothing approaches simplify the margin $M(g, x)$ evaluation by using the bound: $-\max_{k \neq \hat{y}} \tilde{f}_k(x) \geq -(1 - \tilde{f}_{\hat{y}}(x))$ (Cohen et al., 2019). It gives the following certificate for $g = \Phi^{-1} \circ \tilde{f}$:

$$R_2(g, x) \leq R_3(g, x) = \frac{g_{\hat{y}}(x)}{l(g)}. \quad (4)$$

Cohen et al. (2019) motivate the use of certificate R_3 for statistical simplicity and saying that $f(x + \delta)$ puts most of its weight on the top class. For the Carlini et al. (2023) architecture, it is not an optimal choice: in the context of high variance, σ^2 the distribution of $\tilde{f}(x)$ tends to be closer to a uniform distribution. Thus, the difference between radii R_2 and R_3 increases, as shown in Table 3.1. This effect has been noted in Voracek & Hein (2023).

3.2 LOW LIPSCHITZ FOR LOW VARIANCE

The concept of Lipschitz continuity plays an important role in the sampling process, which is crucial for obtaining an accurate estimation of the smoothed classifier \tilde{f} . Specifically, by minimizing the element-wise Lipschitz constant of a classifier f , one can reduce its variance. The following theorem elucidates this correlation for any σ .

Theorem 1 (Gaussian Poincaré inequality (Boucheron et al., 2013)). *Let $Z = (Z_1, \dots, Z_n)$ represent a vector of i.i.d Gaussian random variables with variance σ^2 . For any continuously differentiable function $h : \mathbb{R}^n \rightarrow \mathbb{R}$, the variance is given by:*

$$\mathbb{V}[h(Z)] \leq \sigma^2 \mathbb{E} [\|\nabla h(Z)\|^2].$$

We use the latter theorem to immediately derive:

Corollary 1. *With same hypothesis as Theorem 1, if h exhibits Lipschitz continuity, we have that:*

$$\mathbb{V}[h(Z)] \leq \sigma^2 l(h)^2.$$

Table 1: Comparison of two certified radii R_2 and R_3 , and Total Variation distance to Uniform distribution (TVU), for different values of σ . We took a subset of images from the ImageNet test set with $n = 10^4$, $\alpha = 0.001$, and used Empirical Bernstein inequality. If the effect is not visible for $\sigma < 0.25$, we see that as the TVU decreases, the difference between the two radii increases as well.

σ	TVU	$R_2(g, x)$	$R_3(g, x)$
0.25	0.998	5.89	5.89
0.30	0.996	4.68	4.48
0.35	0.989	3.68	3.21
0.40	0.986	2.49	1.97
0.50	0.976	1.28	0.59
0.60	0.95	0.56	0.00

Applying the above corollary to the classifiers $\{s_k \circ f\}$, it is evident that constraining the Lipschitz constant, $l(s \circ f)$, leads to a diminished variance for $s_k \circ f$. This, in turn, results in a more precise estimation of $\mathbb{E}[s(f(x + \delta))]$, as captured by $\frac{1}{n} \sum_{i=1}^n s(f(x + \delta_i))$. To formalize this relationship, one would need a concentration inequality or an appropriate confidence interval wherein variance plays a significant role. Lowering the local Lipschitz constraints can substantially attenuate variance, producing improved certification results. This is because the compensatory shift, incorporated to address the inherent risk, becomes minimal. However, it is imperative to note that while a globally minimized Lipschitz constraint enhances robustness, it can sometimes be too restrictive, causing a dip in the performance of a classifier designed with Lipschitz constraints. Instead of rigidly constraining the Lipschitz constant by design, softer methods, commonly found in randomized smoothing strategies, have shown better overall performance. For instance, Cohen et al. (2019) proposed the injection of Gaussian noise during training as a means to lower the Lipschitz constant. In a more refined approach, Salman et al. (2019) introduced SmoothAdv, which entails adversarial training for the smoothed classifier \hat{f} , aiming to curtail its local Lipschitz constant. Other noteworthy methods include those by Salman et al. (2020); Carlini et al. (2023), wherein a conventional classifier is combined with a denoiser diffusion model, ensuring that the resulting architecture remains invariant to Gaussian noise, thereby conferring Lipschitz continuity to the classifier.

3.3 STATISTICAL RISK MANAGEMENT IN RANDOMIZED SMOOTHING

RS is a probabilistic procedure, with MC we empirically estimate $\tilde{f}(x) = p$ by \hat{p} . It is necessary to employ a confidence interval or utilize a concentration inequality in order to account for risk at a given significance level α on our estimate p (suppose p in decreasing order). We do as in Levine et al. (2020), the consideration of estimation risk is applied in the form of shifts $\bar{p} = (\hat{p}_1 - \text{shift}_1, \hat{p}_2 + \text{shift}_2, \dots, \hat{p}_c + \text{shift}_c)$. We reorder in decreasing order elements of index $2 \leq i \leq c$ in \bar{p} . The *risk corrected margin* writes as:

$$\bar{M}_1(\hat{p}, \alpha) = \max(0, \bar{p}_1 - \bar{p}_2) \quad \text{or} \quad \bar{M}_2(\hat{p}, \alpha) = \max(0, \Phi^{-1}(\bar{p}_1) - \Phi^{-1}(\bar{p}_2)) , \quad (5)$$

depending if we are using \tilde{f} or $\Phi^{-1} \circ \tilde{f}$ for certification. We also note \bar{R}_1 and \bar{R}_2 the risk-corrected certified radii. Cohen et al. (2019); Salman et al. (2019); Carlini et al. (2023) use argmax simplex projection they can use the *Clopper-Pearson* Bernouilli tailored confidence interval which gives an exact α coverage to determine shift_i . Lecuyer et al. (2019) and Levine et al. (2020) smoothed scalar outputs between within $[0, 1]$ and cannot use such interval, we use the same procedure as those works. They rely upon *Hoeffding's inequality*, which also gives exact α coverage. However, it has some limitations because it does not account for empirical variance. This is why we suggest employing the *Empirical Bernstein's inequality* when the variance is low to manage the risk, α , which does factor in the observed empirical variance.

Proposition 2 (Empirical Bernstein's inequality (Maurer & Pontil, 2009)). *Let Z_0, Z_1, \dots, Z_n be independent and identically distributed random variables with values in $[0, 1]$, and let α be the risk level within $[0, 1]$. With at least a $1 - \alpha$ probability in vector $Z = (Z_1, \dots, Z_n)$, we have*

$$\mathbb{E}Z_0 - \frac{1}{n} \sum_{i=1}^n Z_i \leq \sqrt{\frac{2S_n(Z) \log(2/\alpha)}{n}} + \frac{7 \log(2/\alpha)}{3(n-1)} = \text{shift}(S_n(Z), n, \alpha) .$$

Here, $S_n(Z)$ represents the sample variance $\frac{1}{n(n-1)} \sum_{1 \leq i < j \leq n} (Z_i - Z_j)^2$. Note that the bound is symmetric about $\mathbb{E}Z_0$.

This inequality offers the flexibility to smooth various simplex projections s and potentially select one better equipped than arg max to address the margin-variance tradeoff.

Once the variance has been minimized via Lipschitz constant regularization and that we can leverage low resulting empirical variance with *Empirical Bernstein's inequality* a vital aspect for achieving a significant certified radius is negotiating the margins-variance trade-off. This trade-off arises due to the need to adjust the margin with a shift that incorporates the uncertainty of \hat{g} . Most of RS approaches Cohen et al. (2019), Salman et al. (2019), and Carlini et al. (2023), use the argmax projection choice for simplex projection. Choosing to smooth with the simplex argmax projection can be somewhat arbitrary among all the simplex projections s . In certain cases, it conducts in increased variance as depicted in the following example for s the bi-class argmax projection.

Example 1. For a random variable X defined over the interval $[0, 1]$, with $\mathbb{E}[X] = \frac{1}{2}$ and a "small" variance $\text{Var}[X] = \sigma^2 < \sigma_{\max}^2 = \frac{1}{4}$, define a new random variable as $Y = s(X) = \mathbf{1}_{X > \frac{1}{2}}$. Then $\text{Var}[Y] = \sigma_{\max}^2$ will be much higher than $\text{Var}[X]$ when σ^2 is significantly smaller than $\frac{1}{4}$.

However, argmax projection gives maximum margin on the simplex, as all the mass is put on one class. Conversely, softmax compresses the margins between classes but its 1 -Lipschitz continuity prohibits variance amplifications. Note that argmax is not Lipschitz continuous and cannot provide the same guarantee. Martins & Astudillo (2016) introduced a novel method to project into the simplex. The function $\text{sparsemax}(z) = \arg \min_{p \in \Delta^{c-1}} \|p - z\|_2^2$, a mapping from \mathbb{R}^c to Δ^{c-1} , can also be defined more simply as $\text{sparsemax}(z) = \text{ReLU}(z - \rho)$, the procedure to compute ρ is described in Algo. B.1. This approach promotes sparse outputs in Δ^{c-1} compared to the softmax. It can be considered an alternative to argmax and softmax. It invariably produces margins larger than softmax but lower than argmax. It is 1-Lipschitz so the variance is not increased. Adjusting the temperature t provides a means to interpolate between softmax and argmax, or between sparsemax and argmax. Tuning the temperature allows us to find improved simplex projection to answer the variance-margin trade-off, as illustrated in Figure 2.

3.4 EXPLORING THE INTERPLAY BETWEEN LIPSCHITZ CONTINUITY AND RS

We derive enhanced bounds on the Lipschitz constant of the smoothed classifier \tilde{f} with the additional assumption that $s_k \circ f$ or $s \circ f$ themselves are Lipschitz continuous. Note that one way to have $s \circ f$ or $s_k \circ f$ Lipschitz continuous is to have s Lipschitz continuous as well. This is not the case of argmax simplex projection, whereas sparsemax is ideal as it conserves margin better than softmax and is 1-Lipschitz continuous.

Proposition 3. Let $f : \mathcal{X} \subset \mathbb{R}^d \mapsto \mathbb{R}^c$ a classifier and $\tilde{f}(x) = \mathbb{E}_{\delta \sim \mathcal{N}(0, \sigma^2 I)}[s(f(x + \delta))]$ the associated Gaussian smoothed classifier. Suppose that f is element-wise Lipschitz continuous, then

$$l(\tilde{f}) \leq l(s \circ f) \operatorname{erf}\left(\frac{1}{2^{\frac{3}{2}} l(s \circ f) \sigma}\right) \leq \min\left\{\frac{1}{\sqrt{2\pi\sigma^2}}, l(s \circ f)\right\}. \quad (6)$$

Suppose that f is Lipschitz continuous, then

$$L(\tilde{f}) \leq L(s \circ f) \operatorname{erf}\left(\frac{1}{2L(s \circ f)\sigma}\right) \leq \min\left\{\frac{1}{\sqrt{\pi\sigma^2}}, L(s \circ f)\right\}. \quad (7)$$

We retrieve the factor $\sqrt{2}$ present between $l(\tilde{f})$ and $L(\tilde{f})$ as forecast in Equation (3) between the respective bounds $\frac{1}{\sqrt{2\pi\sigma^2}}$ and $\frac{1}{\sqrt{\pi\sigma^2}}$. It is noteworthy that Equation (6) enhances the bound on $l(\tilde{f})$ originally derived in Lemma 1 of Salman et al. (2019) by a factor of 2. This refinement on the bound was possible by supposing Lipschitz continuity on the *base classifier* f . Note that its Lipschitz constant can be arbitrarily high, so this assumption is quite light. These improved bounds can be seamlessly incorporated into subsequent works, such as Franco et al. (2023). We observe that randomized smoothing and Lipschitz continuity exhibit a cross-effect on the Lipschitz constant of \tilde{f} . We focus on an intermediate regime defined by a specific σ and $l(s \circ f)$, where these effects interact in a manner that is mutually beneficial, exceeding the individual impacts of randomized smoothing or Lipschitz continuity alone.

Proposition 4. For $\gamma \geq 0$, we seek a σ^* that maximizes the gap between the bounds of Equation (6) with respect to σ :

$$\sigma^* = \arg \max_{\sigma > 0} \left\{ \min\left\{\gamma, \frac{1}{\sqrt{2\pi\sigma^2}}\right\} - \gamma \operatorname{erf}\left(\frac{1}{2^{3/2}\gamma\sigma}\right) \right\}.$$

We show that $\sigma^* = \frac{1}{\gamma\sqrt{2\pi}}$.

Using previous result σ^* and substituting it into the bound of \tilde{f} yields:

$$l(\tilde{f}) \leq \operatorname{erf}(\sqrt{\pi}/2) l(s \circ f) \lesssim 0.79 l(s \circ f).$$

Similarly, the same bound applies to $L(\tilde{f})$ when $\sigma^* = \frac{1}{L(s \circ f)\sqrt{\pi}}$. For this choice of σ^* , $l(s \circ f)$ equals the RS bound (and is exactly the deterministic Lipschitz constant). Consequently, the combined use of Lipschitz continuity and randomized smoothing reduces the Lipschitz constant bound

Algorithm 1 LVM-RS

- 1: **input** Trained subclassifier f
- 2: Generate $f(x + \delta_i)$ using MC sampling
- 3: **for** each temperature t
- 4: **for** each simplex projection s
- 5: Compute \hat{p}_{st} , \bar{p}_{st} and $\bar{M}_2(\bar{p}_{st}, \alpha)$
- 6: Choose (s, t) that maximizes $\bar{M}_2(\bar{p}_{st}, \alpha)$ for final classifier
- 7: **output** Prediction and its certificate \bar{R}_2

of \tilde{f} by at most 21%. In our framework, given either a Lipschitz constant (or σ^2), one can select the complementary σ^2 (or Lipschitz constant) to maximize the synergistic effects of randomized smoothing and inherent Lipschitz continuity. For this optimal choice, we obtain a certificate Equation (1) that is approximately 26% larger than the maximum certification given by RS or Lipschitz continuity alone.

3.5 LVM-RS INFERENCE PROCEDURE

Given a trained base subclassifier f , our objective is to assemble an ensemble of smoothed classifiers $\{\tilde{F}_{st}\}$. Here, each classifier is associated with a distinct temperature t and simplex projection s . Formally, each classifier in the ensemble can be represented as:

$$\tilde{F}_s^t(x) = \arg \max_k \mathbb{E}_{\delta \sim \mathcal{N}(0, \sigma^2 I)} [s_k^t(f(x + \delta))] = \arg \max_k \tilde{f}_{st}(x).$$

To estimate $\tilde{f}_{st}(x)$, we employ an MC sampling method, to produce an approximation. Importantly, a single sampling procedure is sufficient as multiple simplex projections can be applied to the $f(x + \delta_i)$ yielding \hat{p}_{st} , for various projections s (spanning softmax and sparsemax) and temperatures t (ranging from t_1 to t_T). For each combination of (s, t) , we determine the risk-corrected margin $\bar{M}_2(\bar{p}_{st}, \alpha)$. Our final classifier is selected based on the (s, t) pairing that maximizes this margin, providing both a prediction and an associated certificate.

Our approach, summed up in Algo. 3.5, innovatively utilizes a single backbone to create an ensemble of classifiers, addressing the inherent tension between maximizing margins and managing variances. This stands in contrast to methods like argmax, which maximize margin at the cost of increased variance, and others like sparsemax and softmax, which prioritize reduced variance over margin maximization.

4 EXPERIMENTS

4.1 CERTIFIED ACCURACY WITH IMPROVED RS LIPSCHITZ

Table 2: Certified accuracy on CIFAR-10 for different levels of perturbation ϵ , for RS network, deterministic Lipschitz network, and ours. The risk is taken as $\alpha = 1e-3$ and the number of samples $n = 10^5$.

Methods	Certified accuracy (ϵ)						Avg. radius
	0.14	0.19	0.25	0.28	0.42	0.5	
Randomized smoothing	60.53	56.62	52.83	50.80	42.03	38.13	0.33
Lipschitz deterministic	60.61	56.72	52.98	50.95	42.16	38.32	0.49
RS with new bound (ours)	62.58	59.44	56.58	54.81	47.25	43.76	0.42

To illustrate the gain of having a Lipschitz bound of *smoothed classifier* which includes information on the Lipschitz constant of *base classifier* and variance σ^2 , we compare certified accuracies on the same by design 1-Lipschitz backbone (Wang & Manchester, 2023) trained with noise injection $\sigma = 0.1$ and using the same certified robust radius in Equation (1) of the following procedures: randomized smoothing, Lipschitz deterministic and our approach. We choose for the smoothing

Table 3: Best certified accuracies across $\sigma \in \{0.25, 0.5, 1.0\}$ for different levels of perturbation ϵ , on CIFAR-10, for $n = 10^5$ samples and risk $\alpha = 1e-3$.

Methods	Best certified accuracy (ϵ)				
	0.0	0.25	0.5	0.75	1.0
Carlini et al. (2023)	86.72	74.41	58.25	40.96	29.91
LVM-RS (Ours)	88.49	76.21	60.22	43.76	32.35

Table 4: Best certified accuracies across $\sigma \in \{0.25, 0.5, 1.0\}$ for different levels of perturbation ϵ , on ImageNet, for $n = 10^4$ samples and risk $\alpha = 1e-3$.

Methods	Best certified accuracy (ϵ)					
	0.0	0.5	1.0	1.5	2	3
Carlini et al. (2023)	79.88	69.57	51.55	36.04	25.53	14.01
LVM-RS (Ours)	80.66	69.84	53.85	36.04	27.43	14.31

variance matching the variance for 1-Lipschitz *base classifier*, *i.e.* $\sigma = \frac{1}{\sqrt{\pi}}$ as explained in Section 3.4. Results are displayed in Table 2. We see that our procedure gives better-certified accuracies than RS and Lipschitz deterministic taken alone. The performance of RS closely mirrors that of deterministic Lipschitz methods. This similarity is anticipated, as when a specific σ is chosen, both methodologies provide an equivalent robustness radius. The primary distinction arises from the risk α embedded within the RS certificate. This risk is responsible for the marginally reduced effectiveness observed in RS and also leads to our average radius being slightly below that of deterministic Lipschitz. Note that better results from the random procedure should not be directly construed as an intrinsic superiority over the deterministic one, as the element of randomness introduces variability that must be accounted for in the evaluation and large sampling computational cost. However, it gives a perspective over the performance of the theoretical Lipschitz *smoothed classifier* \tilde{f} . Results presenting certified radius obtained for $\Phi^{-1} \circ \tilde{f}$ are presented in Table 5.

4.2 CERTIFIED ACCURACIES FOR IMAGE CLASSIFICATION

In this experiment, we empirically validate the efficacy of our proposed inference procedure, highlighting its capability to bolster randomized smoothing and achieve certified accuracy. Central to our approach is the leveraging of the variance-margins tradeoff, which as we demonstrate, yields state-of-the-art RS results. We further showcase how the procedure enhances the off-the-shelf state-of-the-art baseline model of Carlini et al. (2023), which utilizes vision transformers coupled with a denoiser for randomized smoothing. The baseline consists of the state-of-the-art top performative model of Carlini et al. (2023) which does smoothing of argmax of *base classifier* and uses the *Pearson-Clopper* confidence interval to control the risk α .

To compare the baseline with our method, certified accuracies are computed in the function of the level of perturbations ϵ , for different noise levels $\sigma = \{0.25, 0.5, 1\}$. Results are presented in Figure 3 for CIFAR-10 and in Figure 4 for ImageNet. We see that our method increases results, especially in the case of high σ , in the case of $\sigma \in \{0.5, 1.0\}$ the overall certified accuracy curve in the function of ϵ the maximum perturbation is lifted towards higher accuracies. Results are presented in Table 3 for CIFAR-10 and in Table 4 for ImageNet. Detailed results are presented in Appendix C.

5 CONCLUSION

In this paper, we demonstrate a significant correlation between the variance of randomized smoothing and two critical properties of the *base classifier*: its Lipschitz constant and its margin. We highlight the influence of the Lipschitz constant on both the *smoothed classifier* and the empirical variance. To improve the certified robust radius, a novel simplex projection technique is introduced for the *base classifier*, which optimally manages the variance-margin trade-off. Along with this,

we incorporate an advanced Lipschitz bound for the RS, resulting in improved certified accuracy compared to the prevailing methods. In addition, our new certification procedure facilitates the use of pre-trained models in conjunction with randomized smoothing, leading to a direct improvement in the current certification radius.

In future research, we plan to integrate LVM-RS with margin maximization strategies. This combination is expected to improve the robustness of deep neural networks by exploiting LVM-RS's ability to cope with noisy conditions and to strengthen classifier stability through margin expansion.

REFERENCES

Cem Anil, James Lucas, and Roger Grosse. Sorting out lipschitz function approximation. In *International Conference on Machine Learning*, 2019.

Alexandre Araujo, Benjamin Negrevergne, Yann Chevaleyre, and Jamal Atif. On lipschitz regularization of convolutional layers using toeplitz matrix theory. *AAAI Conference on Artificial Intelligence*, 2021.

Alexandre Araujo, Aaron J Havens, Blaise Delattre, Alexandre Allauzen, and Bin Hu. A unified algebraic perspective on lipschitz neural networks. In *International Conference on Learning Representations*, 2023.

Louis Béthune, Thibaut Boissin, Mathieu Serrurier, Franck Mamalet, Corentin Friedrich, and Alberto Gonzalez Sanz. Pay attention to your loss : understanding misconceptions about lipschitz neural networks. In *Advances in Neural Information Processing Systems*, 2022.

Stéphane Boucheron, Gábor Lugosi, and Pascal Massart. *Concentration Inequalities: A Nonasymptotic Theory of Independence*. Oxford University Press, 2013.

Nicholas Carlini, Florian Tramer, Krishnamurthy Dj Dvijotham, Leslie Rice, Mingjie Sun, and J Zico Kolter. (Certified!!) adversarial robustness for free! In *International Conference on Learning Representations*, 2023.

Jeremy Cohen, Elan Rosenfeld, and Zico Kolter. Certified adversarial robustness via randomized smoothing. In *International Conference on Machine Learning*, 2019.

Blaise Delattre, Quentin Barthélémy, Alexandre Araujo, and Alexandre Allauzen. Efficient Bound of Lipschitz Constant for Convolutional Layers by Gram Iteration. In *International Conference on Machine Learning*, 2023.

Nicola Franco, Daniel Korth, Jeanette Miriam Lorenz, Karsten Roscher, and Stephan Guennemann. Diffusion Denoised Smoothing for Certified and Adversarial Robust Out-Of-Distribution Detection. In *arXiv*, 2023.

Miklós Z. Horváth, Mark Niklas Mueller, Marc Fischer, and Martin Vechev. Boosting randomized smoothing with variance reduced classifiers. In *International Conference on Learning Representations*, 2022.

Mathias Lecuyer, Vaggelis Atlidakis, Roxana Geambasu, Daniel Hsu, and Suman Jana. Certified robustness to adversarial examples with differential privacy. In *IEEE symposium on security and privacy (SP)*, 2019.

Alexander Levine, Sahil Singla, and Soheil Feizi. Certifiably robust interpretation in deep learning. In *arXiv*, 2020.

Andre Martins and Ramon Astudillo. From softmax to sparsemax: A sparse model of attention and multi-label classification. In *International Conference on Machine Learning*, 2016.

Andreas Maurer and Massimiliano Pontil. Empirical bernstein bounds and sample variance penalization. *Conference on Learning Theory*, 2009.

Laurent Meunier, Blaise J Delattre, Alexandre Araujo, and Alexandre Allauzen. A dynamical system perspective for lipschitz neural networks. In *International Conference on Machine Learning*, 2022.

Hadi Salman, Jerry Li, Ilya Razenshteyn, Pengchuan Zhang, Huan Zhang, Sébastien Bubeck, and Greg Yang. Provably robust deep learning via adversarially trained smoothed classifiers. *Advances in Neural Information Processing Systems*, 2019.

Hadi Salman, Mingjie Sun, Greg Yang, Ashish Kapoor, and J Zico Kolter. Denoised smoothing: A provable defense for pretrained classifiers. *Advances in Neural Information Processing Systems*, 2020.

Sahil Singla and Soheil Feizi. Fantastic four: Differentiable and efficient bounds on singular values of convolution layers. In *International Conference on Learning Representations*, 2021a.

Sahil Singla and Soheil Feizi. Skew orthogonal convolutions. In *International Conference on Machine Learning*, 2021b.

Christian Szegedy, Wojciech Zaremba, Ilya Sutskever, Joan Bruna, Dumitru Erhan, Ian Goodfellow, and Rob Fergus. Intriguing properties of neural networks. *International Conference on Learning Representations*, 2013.

Asher Trockman and J Zico Kolter. Orthogonalizing convolutional layers with the cayley transform. In *International Conference on Learning Representations*, 2021.

Yusuke Tsuzuku, Issei Sato, and Masashi Sugiyama. Lipschitz-margin training: Scalable certification of perturbation invariance for deep neural networks. *Advances in neural information processing systems*, 2018.

Vaclav Voracek and Matthias Hein. Improving ℓ_1 -Certified Robustness via Randomized Smoothing by Leveraging Box Constraints. In *International Conference on Machine Learning*, 2023.

Ruigang Wang and Ian Manchester. Direct parameterization of lipschitz-bounded deep networks. In *International Conference on Machine Learning*, 2023.

A PROOFS

In this section, for ease of notation, we call h the simplex projection of *base classifier*, *i.e.* $s \circ f$, and \tilde{h} the associated smooth classifier.

A.1 PROOF OF PROPOSITION 3

Proposition. *Let $h : \mathbb{R}^d \mapsto [0, 1]$ a Lipschitz continuous classifier and $\tilde{h}(x) = \mathbb{E}_{\delta \sim \mathcal{N}(0, \sigma^2 I)}[h(x + \delta)]$ the associated Gaussian smoothed classifier. Then,*

$$l(\tilde{h}) \leq l(h) \operatorname{erf} \left(\frac{1}{2^{\frac{3}{2}} l(h) \sigma} \right).$$

Proof. We are interested in the following:

$$J(\sigma, l(h)) = \sup_h \sup_{x \in \mathbb{R}^d} \|\nabla \tilde{h}(x)\| = \sup_h \sup_{x \in \mathbb{R}^d} \sup_{v \in \mathbb{R}^d : \|v\|=1} v^\top \nabla \tilde{h}(x).$$

First, we will derive an upper bound on $J(\sigma, l(h))$. Consider any $x \in \mathbb{R}^d$, any h Lipschitz continuous s.t $h(x) \in [0, 1]$, and any $v \in \mathbb{R}^d$ with $\|v\| = 1$, $u \in \mathbb{R}^c$ with $\|u\| = 1$. Any $\delta \in \mathbb{R}^d$ can be decomposed as $\delta = \delta^\perp + \tilde{\delta}$, where $\tilde{\delta} = (v^\top \delta)v$ and $\delta^\perp \perp v$. Let $\delta' = \delta^\perp - \tilde{\delta}$. That is, δ' is the reflection of the vector δ with respect to the hyperplane that is normal to v . If $\delta \sim \mathcal{N}(0, \sigma^2 I)$, then $\delta' \sim \mathcal{N}(0, \sigma^2 I)$ because $\mathcal{N}(0, \sigma^2 I)$ is radially symmetric. Moreover, $v^\top \delta' = -v^\top \delta$. Hence,

$$\mathbb{E}_{\delta \sim \mathcal{N}(0, \sigma^2 I)}[v^\top \delta h(x + \delta)] = \mathbb{E}_{\delta \sim \mathcal{N}(0, \sigma^2 I)}[v^\top \delta' h(x + \delta')] = -\mathbb{E}_{\delta \sim \mathcal{N}(0, \sigma^2 I)}[v^\top \delta h(x + \delta')].$$

Using the above, we have the following.

$$\begin{aligned} v^\top \nabla \tilde{h}(x) &= \frac{1}{\sigma^2} \mathbb{E}_{\delta \sim \mathcal{N}(0, \sigma^2 I)}[v^\top \delta h(x + \delta)] = \frac{1}{2\sigma^2} \mathbb{E}_{\delta \sim \mathcal{N}(0, \sigma^2 I)}[v^\top \delta(h(x + \delta) - h(x + \delta'))] \\ &\leq \frac{1}{2\sigma^2} \mathbb{E}_{\delta \sim \mathcal{N}(0, \sigma^2 I)}[|v^\top \delta| |h(x + \delta) - h(x + \delta')|] \\ &\stackrel{(i)}{\leq} \frac{1}{2\sigma^2} \mathbb{E}_{\delta \sim \mathcal{N}(0, \sigma^2 I)}[|v^\top \delta| \min\{1, 2l(h)|v^\top \delta|\}] \\ &\stackrel{(ii)}{=} \frac{1}{2\sigma^2} \mathbb{E}_{\delta \sim \mathcal{N}(0, \sigma^2 I)}[|\delta_1| \min\{1, 2l(h)|\delta_1|\}] \\ &\stackrel{(iii)}{=} \frac{1}{2\sigma^2} \mathbb{E}_{z \sim \mathcal{N}(0, \sigma^2)}[|z| \min\{1, 2l(h)|z|\}], \end{aligned}$$

where (i) follows from the Lipschitz assumption on h and the fact that $\|\delta - \delta'\| = \|2\tilde{\delta}\| = \|2(v^\top \delta)v\| = 2|v^\top \delta|$ and that $|h(x + \delta) - h(x + \delta')| \leq 1$, (ii) follows by choosing the canonical unit vector $v = (1, 0, \dots, 0)$ because the previous expression does not depend on the direction of v , and (iii) follows by simply rewriting the expression in terms of z .

Now, we will derive a lower bound on $J(\sigma, l(h))$. For this, we choose a specific $h_o \in [0, 1]$ as $h_o(x) = \operatorname{sign}(x_1) \min\{0.5, l(h)|x_1|\} + 0.5$, with $\operatorname{sign}(0) = 0$, a specific $x = 0$ and specific unit vector $v_0 = (1, 0, \dots, 0)$. For this choice, note that $h_0(0) = 0$ and $v_0^\top \delta = \delta_1$. Then,

$$\begin{aligned} J(\sigma, L) \geq v_0^\top \nabla \tilde{h}_0 &= \frac{1}{\sigma^2} \mathbb{E}_{\delta \sim \mathcal{N}(0, \sigma^2 I)}[v_0^\top \delta h_0(\delta)^\top] = \frac{1}{2\sigma^2} \mathbb{E}_{\delta \sim \mathcal{N}(0, \sigma^2 I)}[|\delta_1| \min\{1, 2l(h)|\delta_1|\}] \\ &= \frac{1}{2\sigma^2} \mathbb{E}_{z \sim \mathcal{N}(0, \sigma^2)}[|z| \min\{1, 2l(h)|z|\}]. \end{aligned}$$

Combining the upper and lower bounds, we have the following equality.

$$J(\sigma, l(h)) = \frac{1}{2\sigma^2} \mathbb{E}_{z \sim \mathcal{N}(0, \sigma^2)} [\min\{|z|, 2l(h)z^2\}]. \quad (8)$$

We will now compute the above expression exactly.

$$\begin{aligned}
\frac{1}{2\sigma^2} \mathbb{E}_{z \sim \mathcal{N}(0, \sigma^2)} [\min \{ |z|, 2l(h)z^2 \}] &= \frac{1}{2\sigma^2} \int_{-\frac{1}{2l(h)}}^{\frac{1}{2l(h)}} \frac{1}{\sqrt{2\pi\sigma^2}} \exp\left(\frac{-z^2}{2\sigma^2}\right) 2l(h)z^2 dz \\
&\quad - \frac{1}{2\sigma^2} \int_{-\infty}^{-\frac{1}{2l(h)}} \frac{1}{\sqrt{2\pi\sigma^2}} \exp\left(\frac{-z^2}{2\sigma^2}\right) z dz \\
&\quad + \frac{1}{2\sigma^2} \int_{\frac{1}{2l(h)}}^{+\infty} \frac{1}{\sqrt{2\pi\sigma^2}} \exp\left(\frac{-z^2}{2\sigma^2}\right) z dz \\
&= \frac{1}{\sigma^2} \int_{-\frac{1}{2l(h)}}^{\frac{1}{2l(h)}} \frac{1}{\sqrt{2\pi\sigma^2}} \exp\left(\frac{-z^2}{2\sigma^2}\right) l(h)z^2 dz + \frac{e^{-\frac{1}{8l(h)^2\sigma^2}}}{2^{\frac{3}{2}}\sqrt{\pi}|\sigma|} + \frac{e^{-\frac{1}{8l(h)^2\sigma^2}}}{2^{\frac{3}{2}}\sqrt{\pi}|\sigma|} \\
&= l(h) \operatorname{erf}\left(\frac{1}{2^{\frac{3}{2}}l(h)\sigma}\right) - \frac{e^{-\frac{1}{8l(h)^2\sigma^2}}}{\sqrt{2}\sqrt{\pi}|\sigma|} + \frac{e^{-\frac{1}{8l(h)^2\sigma^2}}}{2^{\frac{3}{2}}\sqrt{\pi}|\sigma|} + \frac{e^{-\frac{1}{8l(h)^2\sigma^2}}}{2^{\frac{3}{2}}\sqrt{\pi}|\sigma|} \\
&= l(h) \operatorname{erf}\left(\frac{1}{2^{\frac{3}{2}}l(h)\sigma}\right).
\end{aligned}$$

□

Remark 1. Jensen's inequality gives the following simple upper bound on $J(\sigma, l(h))$.

$$\begin{aligned}
J(\sigma, l(h)) &= \frac{1}{2\sigma^2} \mathbb{E}_{z \sim \mathcal{N}(0, \sigma^2)} [\min \{ |z|, 2l(h)z^2 \}] \leq \min \{ \mathbb{E}_{z \sim \mathcal{N}(0, \sigma^2)} [|z|/2\sigma^2], \mathbb{E}_{z \sim \mathcal{N}(0, \sigma^2)} [l(h)z^2/\sigma^2] \} \\
&\leq \min \left\{ \frac{1}{\sqrt{2\pi\sigma^2}}, l(h) \right\}.
\end{aligned}$$

Hence, $J(\sigma, l(h))$ is no worse than the Lipschitz constant of the original classifier f , or its Gaussian smoothed counterpart without the Lipschitz assumption, the latter bound is twice smaller than the previous original derivation.

Proposition. With the same notation as the previous proposition, let $h : \mathbb{R}^d \mapsto \Delta^{c-1}$ a Lipschitz continuous classifier then,

$$J(\sigma, L(h)) = L(h) \operatorname{erf}\left(\frac{1}{2^{\frac{3}{2}}L(h)\sigma}\right).$$

Proof. Here as $h : \mathbb{R}^d \mapsto \Delta^{c-1}$,

$$J(\sigma, L(h)) = \sup_h \sup_{x \in \mathbb{R}^d} \sup_{\substack{v \in \mathbb{R}^d: \|v\|=1 \\ u \in \mathbb{R}^c: \|u\|=1}} v^\top \nabla \tilde{h}(x) u.$$

As in previous proof, consider any $x \in \mathbb{R}^d$, any Lipschitz continuous h s.t $h(x) \in \Delta^{c-1}$, and any $v, u \in \mathbb{R}^d, \mathbb{R}^c$ with $\|v\| = 1$, $\|u\| = 1$, and $\delta = \delta^\perp + \tilde{\delta}$, where $\tilde{\delta} = (v^T \delta)v$ and $\delta^\perp \perp v$. Let $\delta' = \delta^\perp - \tilde{\delta}$.

$$\mathbb{E}_{\delta \sim \mathcal{N}(0, \sigma^2 I)} [v^\top \delta h(x + \delta)^\top u] = \mathbb{E}_{\delta \sim \mathcal{N}(0, \sigma^2 I)} [v^\top \delta' h(x + \delta')^\top u] = -\mathbb{E}_{\delta \sim \mathcal{N}(0, \sigma^2 I)} [v^\top \delta h(x + \delta')^\top u].$$

Using the above, we have the following.

$$\begin{aligned}
v^\top \nabla \tilde{h}(x)^\top v &= \frac{1}{\sigma^2} \mathbb{E}_{\delta \sim \mathcal{N}(0, \sigma^2 I)} [v^T \delta h(x + \delta)^\top u] = \frac{1}{2\sigma^2} \mathbb{E}_{\delta \sim \mathcal{N}(0, \sigma^2 I)} [v^T \delta (h(x + \delta) - h(x + \delta')^\top u)] \\
&\leq \frac{1}{2\sigma^2} \mathbb{E}_{\delta \sim \mathcal{N}(0, \sigma^2 I)} [|v^T \delta| |(h(x + \delta) - h(x + \delta'))^\top u|] \\
&\stackrel{(i)}{\leq} \frac{1}{2\sigma^2} \mathbb{E}_{\delta \sim \mathcal{N}(0, \sigma^2 I)} [|v^T \delta| \min\{\sqrt{2}, 2L|v^T \delta|\}] \\
&\stackrel{(ii)}{=} \frac{1}{2\sigma^2} \mathbb{E}_{\delta \sim \mathcal{N}(0, \sigma^2 I)} [|\delta_1| \min\{\sqrt{2}, 2L|\delta_1|\}] \\
&\stackrel{(iii)}{=} \frac{1}{2\sigma^2} \mathbb{E}_{z \sim \mathcal{N}(0, \sigma^2)} [|z| \min\{\sqrt{2}, 2L|z|\}],
\end{aligned}$$

where (i) follows from the Lipschitz assumption on h and the fact that $\|\delta - \delta'\| = \|2\tilde{\delta}\| = \|2(v^T\delta)v\| = 2|v^T\delta|$ and that $|(h(x+\delta) - h(x+\delta'))^\top u| = \|(h(x+\delta) - h(x+\delta'))^\top u\| \leq \|h(x+\delta) - h(x+\delta')\| \|u\| \leq \sqrt{2}$, (ii) follows by choosing the canonical unit vector $v = (1, 0, \dots, 0)$ because the previous expression does not depend on the direction of v , and (iii) follows by simply rewriting the expression in terms of z .

Now, we will derive a lower bound on $J(\sigma, L(h))$. For this, we choose a specific $\bar{h} \in [0, 1]^C$ as $\bar{h}_1(x) = \text{sign}(x_1) \min\{\frac{\sqrt{2}}{2}, L|x_1|\} + 0.5$, with $\text{sign}(0) = 0$, a specific $x = 0$ and specific unit vectors $\bar{u} = (1, 0, \dots, 0)$, $\bar{v} = (1, 0, \dots, 0)$. For this choice, note that $\bar{h}_1(0) = 0$ and $\bar{v}^\top \delta = \delta_1$. Then,

$$\begin{aligned} J(\sigma, L) \geq \bar{v}^\top \nabla \tilde{h}(0) \bar{u} &= \frac{1}{\sigma^2} \mathbb{E}_{\delta \sim \mathcal{N}(0, \sigma^2 I)} [\bar{v}^\top \delta \bar{h}(\delta)^\top \bar{u}] = \frac{1}{2\sigma^2} \mathbb{E}_{\delta \sim \mathcal{N}(0, \sigma^2 I)} [|\delta_1| \min\{\sqrt{2}, 2L(h)|\delta_1|\}] \\ &= \frac{1}{2\sigma^2} \mathbb{E}_{z \sim \mathcal{N}(0, \sigma^2)} [|z| \min\{\sqrt{2}, 2L(h)|z|\}] . \end{aligned}$$

Combining the upper and lower bounds, we have the following equality:

$$J(\sigma, L(h)) = \frac{1}{2\sigma^2} \mathbb{E}_{z \sim \mathcal{N}(0, \sigma^2)} \left[\min \left\{ \sqrt{2}|z|, 2L(h)z^2 \right\} \right] . \quad (9)$$

We will now compute the above expression exactly.

$$\begin{aligned} \frac{1}{2\sigma^2} \mathbb{E}_{z \sim \mathcal{N}(0, \sigma^2)} \left[\min \left\{ \sqrt{2}|z|, 2L(h)z^2 \right\} \right] &= \frac{1}{2\sigma^2} \int_{-\frac{1}{\sqrt{2L(h)}}}^{\frac{1}{\sqrt{2L(h)}}} \frac{1}{\sqrt{2\pi\sigma^2}} \exp\left(\frac{-z^2}{2\sigma^2}\right) 2L(h)z^2 dz \\ &\quad - \frac{1}{2\sigma^2} \int_{-\infty}^{-\frac{1}{\sqrt{2L(h)}}} \frac{1}{\sqrt{2\pi\sigma^2}} \exp\left(\frac{-z^2}{2\sigma^2}\right) z dz \\ &\quad + \frac{1}{2\sigma^2} \int_{\frac{1}{\sqrt{2L(h)}}}^{+\infty} \frac{1}{\sqrt{2\pi\sigma^2}} \exp\left(\frac{-z^2}{2\sigma^2}\right) z dz \\ &= \frac{1}{\sigma^2} \int_{-\frac{1}{\sqrt{2L(h)}}}^{\frac{1}{\sqrt{2L(h)}}} \frac{1}{\sqrt{2\pi\sigma^2}} \exp\left(\frac{-z^2}{2\sigma^2}\right) L(h)z^2 dz + \frac{e^{-\frac{1}{4L(h)^2\sigma^2}}}{2^{\frac{3}{2}}\sqrt{\pi}|\sigma|} + \frac{e^{-\frac{1}{4L(h)^2\sigma^2}}}{2^{\frac{3}{2}}\sqrt{\pi}|\sigma|} \\ &= L(h) \operatorname{erf}\left(\frac{1}{2L(h)\sigma}\right) - \frac{e^{-\frac{1}{4L(h)^2\sigma^2}}}{\sqrt{2}\sqrt{\pi}|\sigma|} + \frac{e^{-\frac{1}{4L(h)^2\sigma^2}}}{2^{\frac{3}{2}}\sqrt{\pi}|\sigma|} + \frac{e^{-\frac{1}{4L(h)^2\sigma^2}}}{2^{\frac{3}{2}}\sqrt{\pi}|\sigma|} \\ &= L(h) \operatorname{erf}\left(\frac{1}{2L(h)\sigma}\right) . \end{aligned}$$

□

Remark 2. For $h : \mathbb{R}^d \mapsto \Delta^{c-1}$ a Lipschitz classifier, Jensen's inequality gives the following simple upper bound on $J(\sigma, L(h))$.

$$\begin{aligned} J(\sigma, L(h)) &= \frac{1}{2\sigma^2} \mathbb{E}_{z \sim \mathcal{N}(0, \sigma^2)} \left[\min \left\{ \sqrt{2}|z|, 2L(h)z^2 \right\} \right] \\ &\leq \min \left\{ \mathbb{E}_{z \sim \mathcal{N}(0, \sigma^2)} [\sqrt{2}|z|/2\sigma^2], \mathbb{E}_{z \sim \mathcal{N}(0, \sigma^2)} [L(h)z^2/\sigma^2] \right\} = \min \left\{ \frac{1}{\sqrt{\pi\sigma^2}}, L(h) \right\} . \end{aligned}$$

Hence, $J(\sigma, L(h))$ is no worse than the Lipschitz constant of the original classifier h , or its Gaussian smoothed counterpart without the Lipschitz assumption, the latter bound is $\sqrt{2}$ times bigger than the bi-class case with $l(\tilde{h})$.

A.2 PROOF OF PROPOSITION 4

Proposition. For $\gamma \geq 0$, we seek a σ^* that maximizes the gap between the bounds of Equations (6) with respect to σ :

$$\sigma^* = \arg \max_{\sigma > 0} \left\{ \min \left\{ \gamma, \frac{1}{\sqrt{2\pi\sigma^2}} \right\} - \gamma \operatorname{erf}\left(\frac{1}{2^{3/2}\gamma\sigma}\right) \right\} .$$

We show that $\sigma^* = \frac{1}{\gamma\sqrt{2\pi}}$.

Proof. To find the value of σ^* that maximizes the given function, we'll determine the critical points. Let

$$g(\sigma) = \min \left\{ \gamma, \frac{1}{\sqrt{2\pi\sigma^2}} \right\} - \gamma \operatorname{erf} \left(\frac{1}{2^{3/2}\gamma\sigma} \right).$$

Let's start by setting the two functions inside the min function equal to each other and solving for σ :

$$\begin{aligned} \gamma &= \frac{1}{\sqrt{2\pi\sigma^2}} \\ \Rightarrow \sigma^2 &= \frac{1}{\gamma^2 2\pi} \\ \Rightarrow \sigma &= \frac{1}{\gamma\sqrt{2\pi}}. \end{aligned}$$

This is the point of intersection, hence the value of σ where the two functions inside the min change dominance. For that value, $g(\frac{1}{\gamma\sqrt{2\pi}}) = \gamma(1 - \operatorname{erf}(\frac{\sqrt{\pi}}{2}))$.

Now, for $\sigma < \frac{1}{\gamma\sqrt{2\pi}}$, $g(\sigma) = \gamma - \gamma \operatorname{erf} \left(\frac{1}{2^{3/2}\gamma\sigma} \right)$.

Let's differentiate $g(\sigma)$ in the this first region:

$$\begin{aligned} g'(\sigma) &= 0 - \frac{d}{d\sigma} \left[\gamma \operatorname{erf} \left(\frac{1}{2^{3/2}\gamma\sigma} \right) \right] \\ &= \gamma \frac{1}{2^{3/2}\gamma} \frac{2}{\sqrt{\pi}} \exp \left(- \left(\frac{1}{2^{3/2}\gamma\sigma} \right)^2 \right) \\ &= \frac{1}{\sqrt{2\pi}} \exp \left(- \left(\frac{1}{2^{3/2}\gamma\sigma} \right)^2 \right). \end{aligned}$$

The supremum is obtained for $\sigma \rightarrow 0$, and the associated limit value for $g(\sigma)$ is 0.

For the second region, $\sigma > \frac{1}{\gamma\sqrt{2\pi}}$, $g(\sigma) = \frac{1}{\sqrt{2\pi\sigma^2}} - \gamma \operatorname{erf} \left(\frac{1}{2^{3/2}\gamma\sigma} \right)$. Supremum is obtained for $\sigma \rightarrow \frac{1}{\gamma\sqrt{2\pi}}$ as g is a decreasing function of σ . The associated limit value for $g(\sigma)$ is $\gamma(1 - \operatorname{erf}(\frac{\sqrt{\pi}}{2}))$.

Finally, $\sigma^* = \frac{1}{\gamma\sqrt{2\pi}}$ gives maximum value for g on all domain.

□

A.3 PROOF OF EXAMPLE 1

Example. For a random variable X defined over the interval $[0, 1]$, with $\mathbb{E}[X] = \frac{1}{2}$ and a "small" variance $\operatorname{Var}[X] = \sigma^2 < \sigma_{\max}^2 = \frac{1}{4}$, define a new random variable as $Y = s(X) = \mathbb{1}_{X > \frac{1}{2}}$. Then $\operatorname{Var}[Y] = \sigma_{\max}^2$ will be much higher than $\operatorname{Var}[X]$ when σ^2 is significantly smaller than $\frac{1}{4}$.

Proof. Let us compute $\mathbb{E}[Y]$, since Y is an indicator random variable, we have: $\mathbb{E}[Y] = \mathbb{P}(Y = 1) = \mathbb{P}(X > \frac{1}{2})$. Given X is symmetric around 0.5, we find $\mathbb{E}[Y] = 0.5$. The variance of Y is given by: $\mathbb{V}[Y] = \mathbb{E}[Y^2] - (\mathbb{E}[Y])^2$. Since Y is an indicator variable, $Y^2 = Y$, and therefore $\mathbb{E}[Y^2] = \mathbb{E}[Y] = 0.5$. Thus, we have: $\mathbb{V}[Y] = 0.5 - 0.25 = 0.25$. To claim that $\mathbb{V}[Y]$ has a much higher variance than $\mathbb{V}[X]$, we need to compare 0.25 to σ^2 . The statement would be true if σ^2 is substantially smaller than 0.25. Given that X is defined over $[0, 1]$ and its mean is 0.5, the variance of X could range between 0 and 0.25. Therefore, unless X has a variance near this upper bound, $\mathbb{V}[Y]$ will indeed be much larger. □

B SPARSEMAX

B.1 SPARSEMAX ALGORITHM

Algorithm 2 Sparsemax

- 1: **input** z
- 2: Sort z as $z^{(1)} \geq \dots \geq z^{(K)}$
- 3: Find $k(z)$ such that

$$k(z) = \max_{k \in [K]} \left\{ k \left| 1 + kz^{(k)} > \sum_{j \leq k} z^{(j)} \right. \right\}$$

- 4: Define

$$\rho(z) = \frac{\sum_{j \leq k(z)} z^{(j)}}{k(z)}$$

- 5: **output** p such that $p_i = \max(z_i - \rho(z), 0)$

B.2 ADDRESSING VARIANCE-MARGIN TRADEOFF WITH SIMPLEX PROJECTION

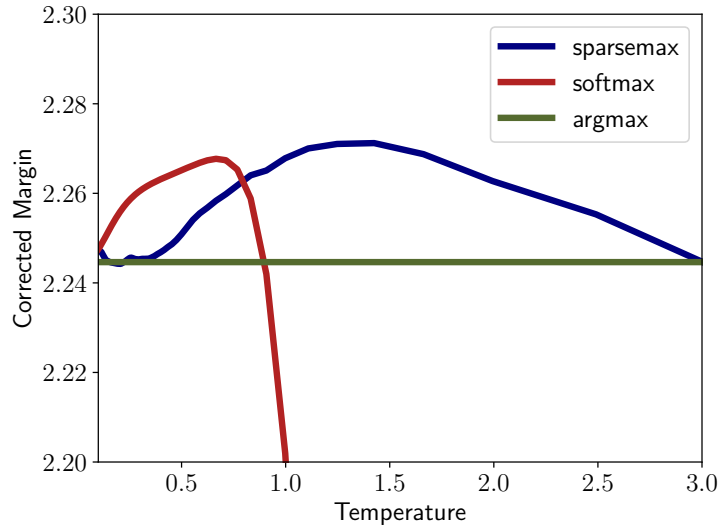


Figure 2: Comparison of the effect on corrected margin of the choice of the simplex projection s and associated temperature t . Margin is risk corrected with Empirical Bernstein inequality for a risk $\alpha = 1e-3$ and $n = 10^4$, the same certified robust radius is used. The *base classifier* is the one from Carlini et al. (2023) and margins were generated with one image from ImageNet. Simplex projections considered are $s \in \{\text{argmax}, \text{softmax}, \text{sparsemax}\}$. We see that by varying the temperature t , softmax and sparsemax are able to find a better solution than argmax to the variance-margin trade-off.

C FIGURES AND TABLES FOR EXPERIMENTS

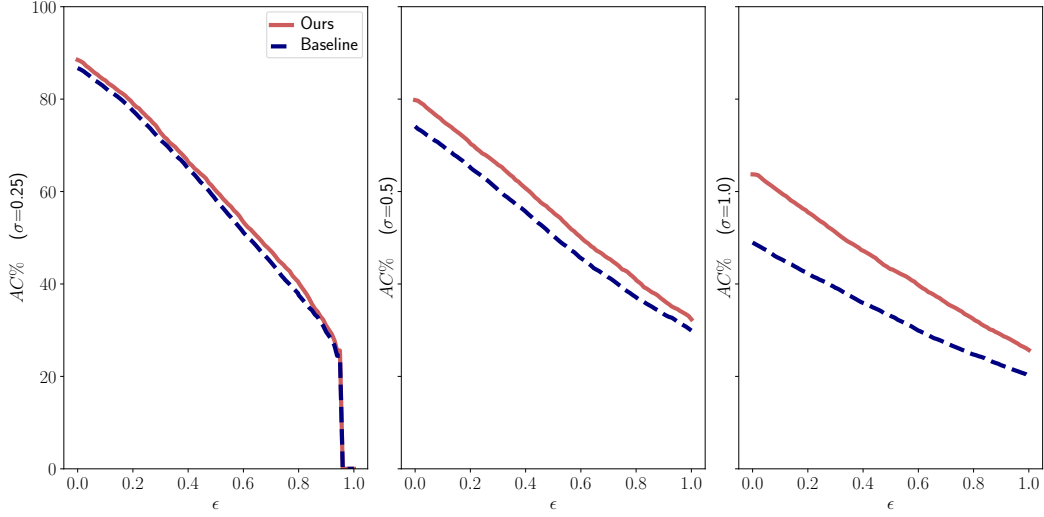


Figure 3: Certified accuracies (CA in %) in function of level of perturbations ϵ on CIFAR-10, for different noise levels $\sigma = \{0.25, 0.5, 1\}$. Number of samples is $n = 10^5$ and risk $\alpha = 1e-3$. Our method is compared to the baseline chosen as in Carlini et al. (2023).

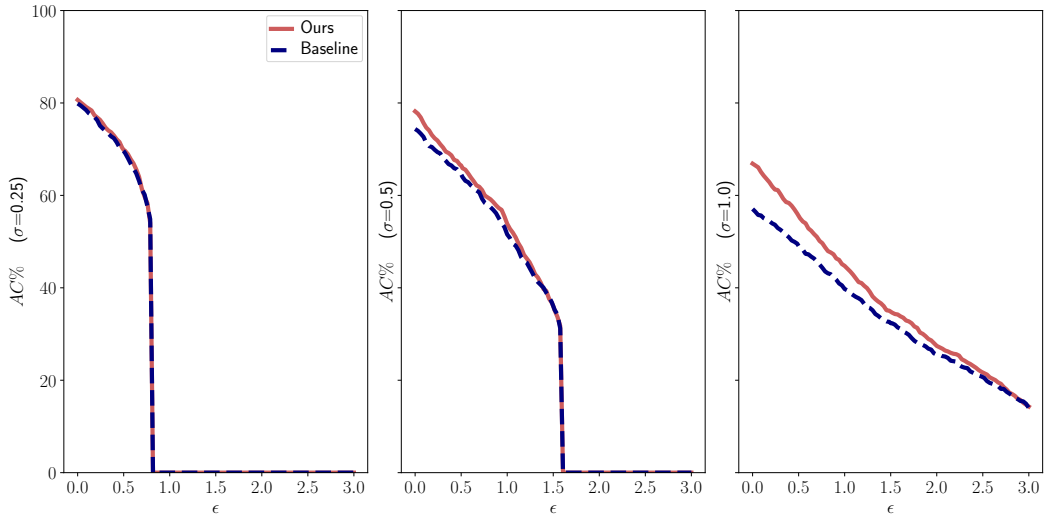


Figure 4: Certified accuracies (CA in %) in function of level of perturbations ϵ on ImageNet, for different noise levels $\sigma = \{0.25, 0.5, 1\}$. Number of samples is $n = 10^4$ and risk $\alpha = 1e-3$. Our method is compared to the baseline chosen as in Carlini et al. (2023).

Table 5: Certified accuracy on CIFAR-10 for different levels of perturbation ϵ , for RS network, deterministic Lipschitz network, and ours. The risk is taken as $\alpha = 1e-3$ and the number of samples $n = 10^5$. Here we use certified radius Eq. (1) for Lipschitz Deterministic, the radius with $\Phi^{-1} \circ \tilde{f}$ Eq. (2) for RS and the maximum of both for ours.

Methods	Certified accuracy (ϵ)						Average radius
	0.14	0.19	0.25	0.28	0.42	0.5	
Randomized smoothing	60.93	57.20	53.65	51.74	44.33	41.03	0.73
Lipschitz deterministic	60.61	56.72	52.98	50.95	42.16	38.32	0.49
RS with new bound (ours)	62.58	59.44	56.58	54.81	47.25	43.76	0.75

Table 6: Certified accuracies comparison for different perturbation ϵ values, for $n = 10^4$ samples and $\alpha = 1e-3$. On ImageNet dataset. Here the baseline is a ResNet 150 from Salman et al. (2019).

Methods	Certified accuracy (ϵ)							
	0.14	0.2	0.3	0.4	0.5	0.6	0.7	0.8
Salman et al. (2019)	74.49	73.08	69.84	66.41	62.42	57.75	51.24	0.0
LVM-RS (Ours)	76.77	74.99	71.26	67.55	63.43	58.59	51.39	0.0

Table 7: Certified accuracy for $\sigma = 0.25$ on CIFAR-10, for risk $\alpha = 1e-3$ and $n = 10^5$ samples.

Methods	Epsilon										
	0.0	0.14	0.2	0.25	0.3	0.4	0.5	0.6	0.75	0.8	1.0
Carlini et al. (2023)	86.72	80.73	77.47	74.41	71.15	65.01	58.25	51.15	40.96	37.6	0.0
LVM-RS (Ours)	88.49	82.15	79.06	76.21	72.73	66.41	60.22	53.41	43.76	40.27	0.0

Table 8: Certified accuracy for $\sigma = 0.5$ on CIFAR-10, for risk $\alpha = 1e-3$ and $n = 10^5$ samples.

Methods	Epsilon										
	0.0	0.14	0.2	0.25	0.3	0.4	0.5	0.6	0.75	0.8	1.0
Carlini et al. (2023)	74.11	67.99	65.22	62.89	60.38	55.67	50.43	45.59	39.26	37.11	29.91
LVM-RS (Ours)	79.79	73.45	70.41	68.04	65.8	60.71	55.48	50.07	43.13	40.83	32.35

Table 9: Certified accuracy for $\sigma = 1$ on CIFAR-10, for risk $\alpha = 1e-3$ and $n = 10^5$ samples.

Methods	Epsilon										
	0.0	0.14	0.2	0.25	0.3	0.4	0.5	0.6	0.75	0.8	1.0
Carlini et al. (2023)	48.97	44.24	42.26	40.76	39.15	35.91	33.08	29.92	25.97	24.72	20.09
LVM-RS (Ours)	63.72	57.99	55.54	53.4	51.23	47.19	43.19	39.76	34.27	32.35	25.71

Table 10: Certified accuracy for $\sigma = 0.25$ on ImageNet, for risk $\alpha = 1e-3$ and $n = 10^4$ samples.

Methods	Epsilon					
	0.0	0.5	1.0	1.5	2	3
Carlini et al. (2023)	79.88	69.57	0.0	0.0	0.0	0.0
LVM-RS (Ours)	80.66	69.84	0.0	0.0	0.0	0.0

Table 11: Certified accuracy for $\sigma = 0.5$ on ImageNet, for risk $\alpha = 1e-3$ and $n = 10^4$ samples.

Methods	Epsilon					
	0.0	0.5	1.0	1.5	2	3
Carlini et al. (2023)	74.37	64.56	51.55	36.04	0.0	0.0
LVM-RS (Ours)	78.18	66.47	53.85	36.04	0.0	0.0

Table 12: Certified accuracy for $\sigma = 1$ on ImageNet, for risk $\alpha = 1e-3$ and $n = 10^4$ samples.

Methods	Epsilon					
	0.0	0.5	1.0	1.5	2	3
Carlini et al. (2023)	57.06	49.05	39.74	32.33	25.53	14.01
LVM-RS (Ours)	66.87	55.56	44.74	34.83	27.43	14.31